



Ultrasound treatment to improve encapsulation efficiency of curcumin in alginate/carrageenan beads

Aji Prasetyaningrum, Nur Rokhati, Moh Djaeni, Bakti Jos, Ratnawati, Azafilmi Hakiim, Aulia Dwi Ashianti, and Sadrah Farel Christian Manalu

University of Diponegoro, Faculty of Engineering, Jl. Prof. Soedarto SH, Tembalang, Semarang, Indonesia.

Abstract

This study aims to investigate the effect of ultrasound treatment on curcumin encapsulation in alginate/carrageenan beads to improve its stability and bioavailability. The functional groups of microcapsules were analyzed using Fourier Transform Infrared Spectroscopy (FTIR) and their morphology was characterized using a Scanning Electron Microscope (SEM), besides that the particle distribution was measured using a Particle Size Analyzer (PSA). The FTIR results show that the ultrasound treatment has a small effect in the form of a peak shift (1266 cm^{-1}) which indicates the breaking of the C-H bond and results in polymer degradation. The SEM results show that ultrasonication causes explosions and cracks on the particle walls. The PSA results show that ultrasonication reduces the particle size to $51.26\text{ }\mu\text{m}$. In this study, the use of ultrasound can increase the encapsulation efficiency from 95% to 98%. However, prolonged sonication causes the efficiency to decrease. This is because the excessive sonication process makes the bonds break. Increasing the concentration of CaCl_2 as a crosslinker agent causes the swelling ratio to decrease due to the stronger bonding of Ca^{2+} with alginate/carrageenan beads. The release of bioactives from the ultrasound-treated beads is controlled more by diffusion mechanisms than by relaxation. This study shows that ultrasound treatment is successfully used in curcumin encapsulation process.

Keywords: sonication, microcapsule, bioactive, polymer, material

Full length article *Corresponding Author, e-mail: aji.prasetyaningrum@che.undip.ac.id

1. Introduction

Turmeric is an herbal plant known for its medicinal properties to treat various disorders in traditional Asian medicine [1]. Depending on its origin and soil conditions, turmeric contains between 2 and 9% curcuminoids - a group of compounds including curcumin, as the major component, demethoxycurcumin, and bisdemethoxy-curcumin [2]. Curcumin (Cur) has a number of beneficial biological and pharmacological properties, including anti-inflammatory, anti-bacterial, anti-oxidant, anti-viral, and anti-cancer [3]. Although curcumin (Cur) has a wide range of functional activities, its application in the food and pharmaceutical industries is limited due to its higher hydrophobicity, lower oral utilization and poor stability [4]. Various methods have been used to stabilize curcumin, avoiding significant discoloration and the bioavailability of bioactive compounds. The technology most often used to protect and provide the expected properties of active substances is encapsulation. Encapsulation is a method of entrapment of active compounds into the outer layers or matrix. It helps to improve solubility, controlled release, uniform distribution of core material, and bioavailability of bioactives [5]. The encapsulating substance is known as the shell, carrier, wall

material, or outer phase, whereas the substance being encapsulated is known as the core material, active substance, or internal phase. Wall material is one thing that has an important role in the encapsulation process [6]. The most commonly used encapsulants are polysaccharides [7]. Alginate (Alg) is a natural polymer extracted from brown seaweed and has a negative charge consisting of 1,4-linked β -D-mannuronic acid and 1,4- α -L-guluronic acid [8]. Alginate (Alg) has become the most commonly used encapsulant in encapsulation because of its biocompatibility, low toxicity, and relatively low cost [9]. However, Alg can provide obstacles in its application, namely high permeability to water-soluble compounds in the encapsulation process. This problem can be prevented by mixing Alg with other encapsulating agents [10]. One of the polymers that can be combined with Alg is carrageenan.

Carrageenan (Carr) is also a class of polysaccharides obtained from red algae [11]. The addition of κ -carrageenan tends to also improve the gel moisture content, elastic modulus, thermal properties and swelling induced by the sulfate groups of Carr molecules [12]. The Alg/Carr combination as a wall material was successfully used by Gu

et al (2020) to encapsulate egg yolk immunoglobulin Y [13]. That study showed that Alg/Carr beads were suitable for use as a wall material for encapsulation.

The methods commonly used for the encapsulation of bioactive compounds are spray drying, freeze drying, extrusion, microemulsion, coacervation, ionic gelation, and other methods [14]. Encapsulation using ionic gelation method is a promising method because it is a simple and easy procedure. Ionic gelation is an attractive technique, because it can be considered low-cost and does not require special equipment, high temperatures, and organic solvents [15]. However, the disadvantage of ionic gelation is its low mechanical stability. Emulsion formation requires an input of energy to blend two immiscible liquids when the proper emulsifier is not added to the mixture. Problems with these limitations can be overcome using ultrasound treatment.

The use of ultrasonication technology assistance can be a solution to minimize the resulting deficiencies when only using the ionic gelation method. Ultrasonication is a technology with proven effectiveness for preparing various catalytic and functional materials that can be applied in various fields [16]. The emulsion's droplet size can be reduced to nanometer size with ultrasound treatment [17]. Additionally, ultrasound can speed up homogenization. Due to the reduced droplet size of the emulsion, the bioactive encapsulation in the wall material will increase [18]. Ultrasound treatment using high frequency (<20 kHz) sonic waves will produce agitation which is useful in microcapsule formation [18]. The agitation phenomenon will create a gas or liquid cavity in an explosive system. The collapsing cavitation waves cause the H₂O bonds to break and produce free radicals. This in turn triggers the ability to form microcapsules [16]. The ultrasound procedure does not affect the functional properties of the core or wall material and improves the stability of the material. Ultrasound is one of the promising techniques for preparing stable core-wall materials with controlled physical and biofunctional properties using conventional methods.

Since research on the ultrasound-assisted encapsulation of curcumin (Cur) using Alg/Carr is limited, the objective of this study was to encapsulate Cur into polysaccharide (Alg/Carr) particles in order to increase its stability and bioavailability. The porosity of the polymer matrix can be controlled by varying the times of ultrasonication and crosslinker agent concentration. The particles obtained were characterized morphologically by scanning electron microscopy (SEM), functional groups by FTIR spectroscopy. The bioactive release kinetic behaviour was also studied for further studies of controlled release.

2. Materials and methods

2.1. Materials

Curcumin (95% purity) was procured from Sigma-Aldrich. Other chemicals used were sodium alginate (molar mass 216.12 g/mol with CAS number 9005-38-3 SIGMA-Aldrich, USA), carrageenan, CaCl₂, HCl, NaOH, and buffer solution (Merck Chemical Co, Darmstadt, Hesse, Germany). All chemicals used analytical grade.

2.2. Preparation of the complex particles

The manufacture of microcapsules containing curcumin refers to research conducted by Elgeggen et al (2019) and Iurciuc-Tincu et al (2020) with several modifications [19, 20]. The curcumin microcapsules were prepared in 2 step. The first step is to make an alginate solution by dissolving 2% (w/v) sodium alginate in distilled water and stirring using a magnetic stirrer. Next, dissolve 1% (w/v) carrageenan in distilled water and homogenize with a magnetic stirrer. Mix the two solutions and homogenize for 30 minutes. The second step, prepare a curcumin solution by dissolving 0.5% (w/v) curcumin in soybean oil. Add curcumin solution to the alginate/carrageenan mixture and homogenize. Next, the mixed solution is sonicated. The ultrasonication time was varied: 0, 4, 6, 8, 10 and 12 minutes. Then, the emulsion formed was dropped with a syringe into a solution of CaCl₂ with a concentration of 0.2M. The mixture will form beads in CaCl₂ solution, wait 30 minutes. Filter the beads, and dry them in a drying tray at 27°C for 48 hours.

2.3. Characterization of the particles

2.3.1. Encapsulation Efficiency

Encapsulation efficiency was carried out by determining the amount of bioactive that was not trapped in the Alg/Carr beads after being dropped into the CaCl₂ solution. In this case, the encapsulation efficiency is:

$$EE (\%) = \frac{Q_t - Q_r}{Q_t} \times 100\% \quad (1)$$

where Q_t is the amount of bioactive curcumin and Q_r is the bioactive curcumin present in CaCl₂ solution after encapsulation.

2.3.2. Swelling Test

The swelling test was carried out in a buffer solution at pH 1.2 and 6.8. The percentage of swelling can be calculated using the equation:

$$Swelling = \frac{W_s - W_d}{W_d} \quad (2)$$

W_s is the weight of wet beads and W_d is the weight of dry beads.

2.3.3. Particle Size Analysis (PSA)

Determination of particle size using a laser particle size analyzer Labtron LLPA-C10. The sample is weighed and then put into a cuvette and added with aqua pro injection. After that, the cuvette was inserted into the holder of the PSA tool.

2.3.4. Scanning Electron Microscope (SEM) Analysis

The morphology of curcumin, alginate/carrageenan, and encapsulated beads was observed with JEOL JSM-6510LA SEM. The samples were coated with gold using a sputter coating equipment before analysis.

2.3.5. Fourier Transform Infrared Spectroscopy (FTIR) Analysis

The functional groups of curcumin, alginate/carrageenan, and encapsulated beads were studied by recording IR absorption data between 4000 and 500 cm^{-1} using a Perkin Elmer Spectrum IR 10.6.1 spectrophotometer at room temperature.

3. Results and Discussions

3.1. Fourier Transform Infrared Spectroscopy (FTIR)

The functional groups of the curcumin encapsulated product were analyzed using FTIR. The FTIR spectra of the ultrasonic-assisted microcapsules were compared to the unassisted microcapsules, empty alginate-carrageenan granules, and curcumin for precise and thorough analysis.

The FTIR spectra of curcumin in Figure 2a shows infrared absorption at a wavelength of 2922 cm^{-1} (O-H) indicating a free phenolic hydroxyl group, the peak at a

wavelength of 1633 cm^{-1} (C=O) indicates an aliphatic chain, band 1513 cm^{-1} (C=C) of the aromatic chain, 1325 cm^{-1} (=C-O-C), 1149 cm^{-1} (C-O-C), and 1075 cm^{-1} (C-O) of the ether attached to the aromatic ring, and the alcohol group 1372 cm^{-1} (C-O-H) is attached to the aromatic ring. The band at 996 cm^{-1} (C-H) corresponds to an alkene. This kind of phenomenon was also observed in a study by Chen et al. (2021) [21].

Furthermore, in Figure 2b of the spectrum of alginate added to carrageenan, the absorbance at 888.02 cm^{-1} is a group of the anomeric C-H β -galactopyranose. There is a peak at 1417.03 cm^{-1} which is an extension of the S=O sulfate group which is the carrageenan. There is also a strong band at 1023.32 cm^{-1} which is due to the stretching vibration of the C-O bond. An absorption band is also present at 1594.60 cm^{-1} resulting from the asymmetric and symmetric vibrations of the carboxylate anion present in the alginate.

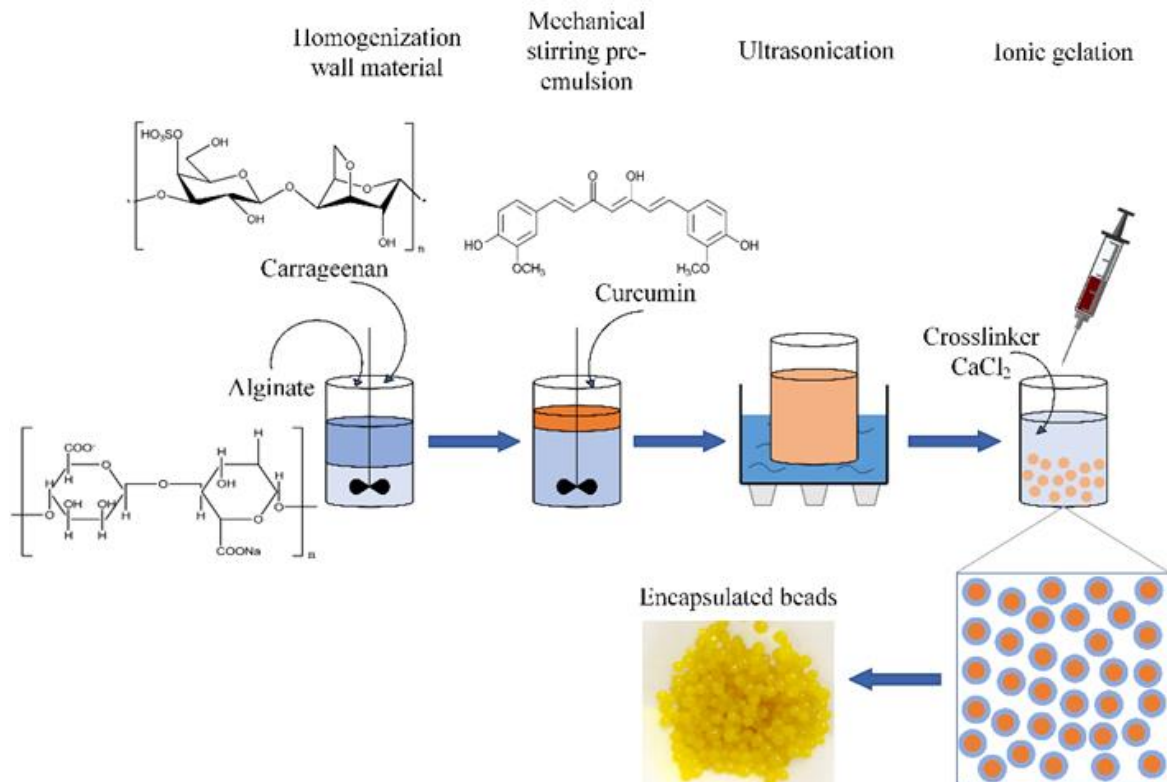


Figure 1. Experimental set-up

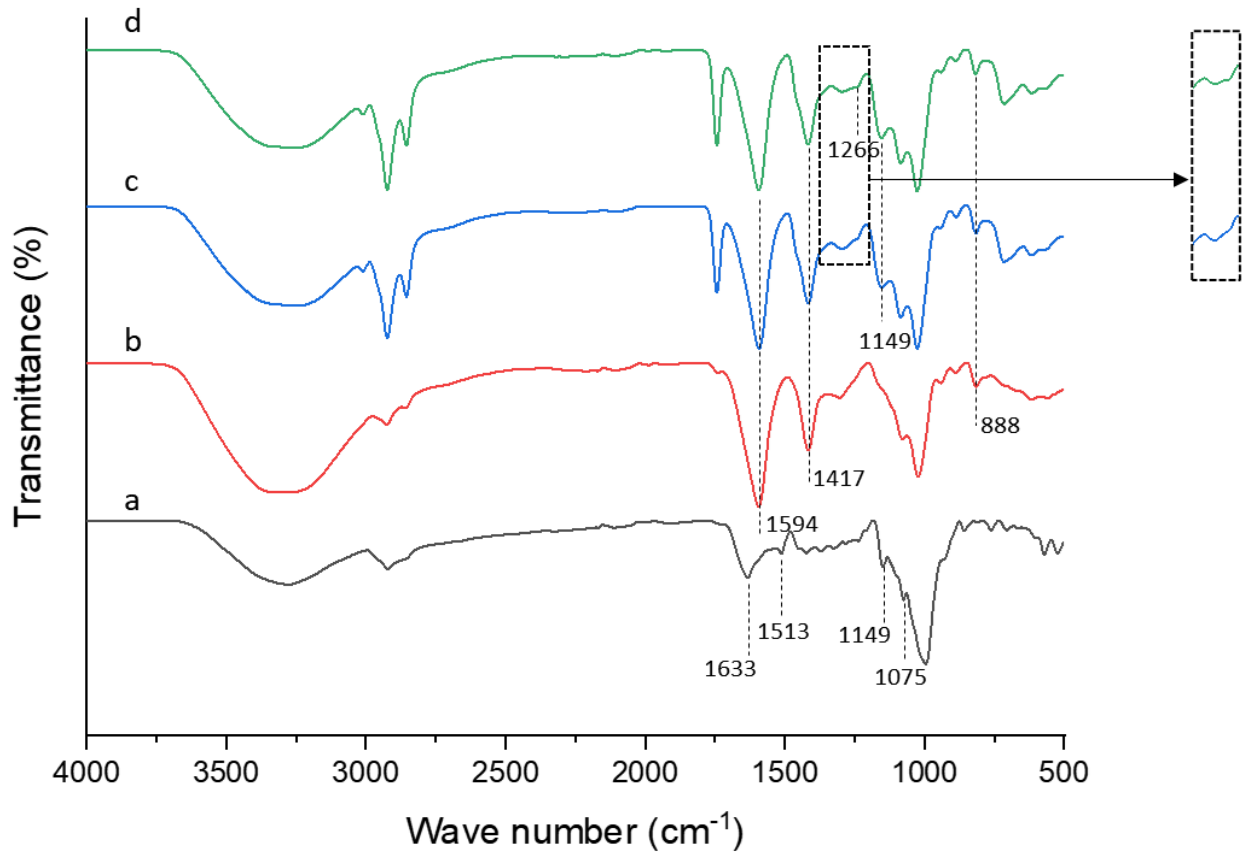


Figure 2. FTIR spectra for a) Curcumin; b) Alg/Carr; c) Alg/Carr/Cur (Non-Ultrasound); d) Alg/Carr/Cur (Ultrasound)

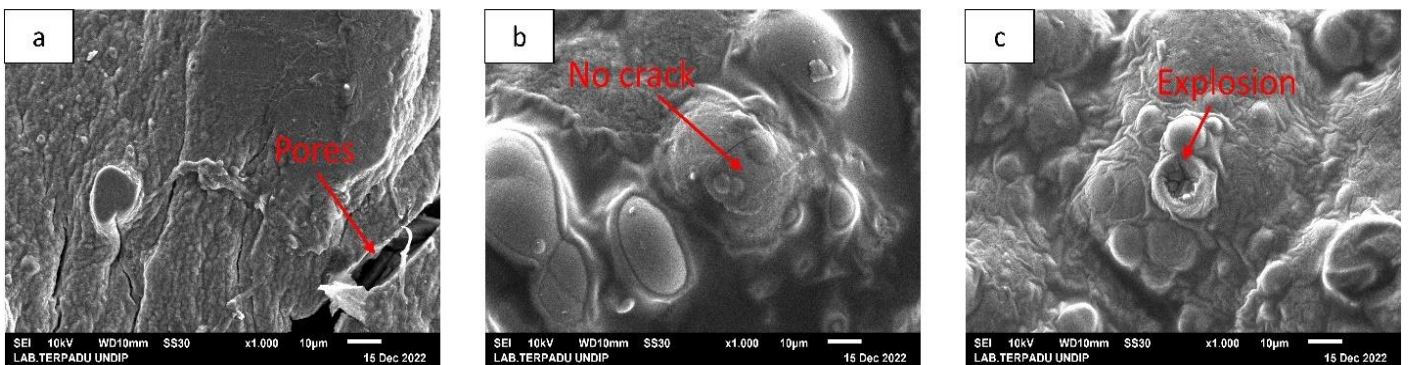


Figure 3. SEM images of encapsulation curcumin beads: a) Alg/Carr; b) Alg/Carr/Cur/Non-Ultrasound; c) Alg/Carr/Cur/Ultrasound

In Figures 2c and 2d we can see that the encapsulation properties of curcumin have little impact on the ultrasonically assisted functional groups. Figure 2d shows that the spectrum of ultrasonically-assisted curcumin in alginate/carrageenan matrix has a peak shift at 1266 cm^{-1} indicating bond breaking. The ultrasonic process causes the C-H bonds to break, leading to degradation of the polymer. This is consistent with the research by Liang et al. (2018) [22].

3.2. Scanning Electron Microscope (SEM)

SEM images showing the surface morphology of the particles at 1000x magnification are presented in Figure 3. From Figure 3a it can be seen that the Alg/Carr beads have a pore structure on their surface. This effect can be attributed to the higher cross-linking ability of alginate than carrageenan. The crosslinking process occurs when alginate enters the crosslinking solution (consisting of Ca^{2+}) resulting stable particles. Thus, formulations containing carrageenan, the beads are less round, have a rough and folded surface [23].

Figures 3b and 3c show that the ultrasonication process gives different morphologies to the formed beads. The SEM results show damage to the surface of the sample beads by ultrasound treatment, which can be observed as explosions and cracks. The cavitation phenomenon, which generates extremely high stresses and shear forces, can lead to damage on the surface of the beads. This mechanical degradation of the amorphous layer wall material reduces the particle size, particularly resulting in several gaps and cracks on the surface of the beads. As a result of this occurrence, the alginate carboxyl groups and glycosidic linkages break down, resulting in a looser particle structure that allows more room for the surrounding medium to penetrate the particles. Similar results were also shown in previous research conducted by Prasetyaningrum et al. (2023) [24].

3.3. Particle Size Analyzer (PSA)

Characterization using PSA aims to measure the particle size distribution. The particle size of beads are shown in Table 1. At 0 min ultrasonic time (without ultrasound) obtained a particle size of $70.78\ \mu\text{m}$. The encapsulation product was given a particle size of $51.26\ \mu\text{m}$ with the treatment of ultrasound for 12 minutes. In general, ultrasound causes particle size reduction due to the formation of denser particle structures [25]. In ultrasound, the shear force generated by the bursting of bubbles generated by the acoustic cavity can break down large polymers that form to reduce particle size [16]. The cavitation effect also has several other effects on particle deaggregation. According to previous studies, the generation of a bubble cloud can reduce the amount of acoustic pressure that is emitted through the liquid medium, decreasing the ultrasonic field around the conical bubble structure. [26]. The collapse of cavitation bubbles can generate powerful shock waves and extremely high pressure. Ultrasound can also reduce the influence of polarity on the solution and increase its solubility, thus effectively reducing the average size of the nanoparticles and stabilizing the colloidal system [27].

Table 1: Particle size at various ultrasound time

| Ultrasound time (min) | Diameter (μm) |
|-----------------------|----------------------------|
| 0 | 70.78 |
| 4 | 67.48 |
| 6 | 64.81 |
| 8 | 62.15 |
| 10 | 57.95 |
| 12 | 51.26 |

3.4. Encapsulation Efficiency

3.4.1. Effect Ultrasonic Time

As shown in Figure 4, ultrasound time has an effect on encapsulation efficiency. Encapsulation efficiency increases from 0 to 8 minutes. the best conditions were obtained with an encapsulation efficiency of 98.29%. Furthermore, the encapsulation efficiency decreased from 8 to 12 minutes. This could occur because the ultrasonication process can open the polysaccharide structure of the wall material. In addition, this phenomenon is also caused by more broken glycosidic bonds. However, excessive ultrasound treatment can cause polysaccharides to unfold and aggregation resulting in decreased encapsulation efficiency. Sonication can reduce the particle size and increase the surface area so that the coating process will be easier and the encapsulation efficiency will increase. On the other hand, a long sonication process can reduce encapsulation efficiency. Excessive sonication causes polymer degradation and shortens polymer chains thereby affecting the strength of intermolecular bonds and the ability of Alg/Carr to retain curcumin also decreases. This phenomenon is similar to research conducted by Luo et al. (2022) [27].

3.4.2. CaCl_2 Concentration

As shown in Figure 5, encapsulation efficiency of Alg/Carr beads for curcumin was also significantly increased by the addition of CaCl_2 . The lowest encapsulation efficiency occurred at 0.1M CaCl_2 concentration of 91.11%, and the highest at 0.3M concentration of 93.97%. The role of the cross-linking agent is important for the hardening of the coating material. When the concentration of CaCl_2 increases, the availability of Ca^{2+} ions also increases, which causes stronger cross-linking of the alginate-carrageenan matrix, thereby providing more trapped bioactive compounds of curcumin. The same thing also happened in the research by Tunsirikongkon et al. (2020) [28].

3.6. Release Kinetic

According to the results of the experiment, there is a lower percentage of curcumin release at pH 1.2 (Figures a and b) than at pH 6.8 (Figures c and d). This is also demonstrated in Table 2, where the release rate, or k value, is lower at pH 1.2 than it is at pH 6.8. Due to the formation of carboxyl ion groups, alginate dissolves more readily at higher pH levels, which causes this phenomena.

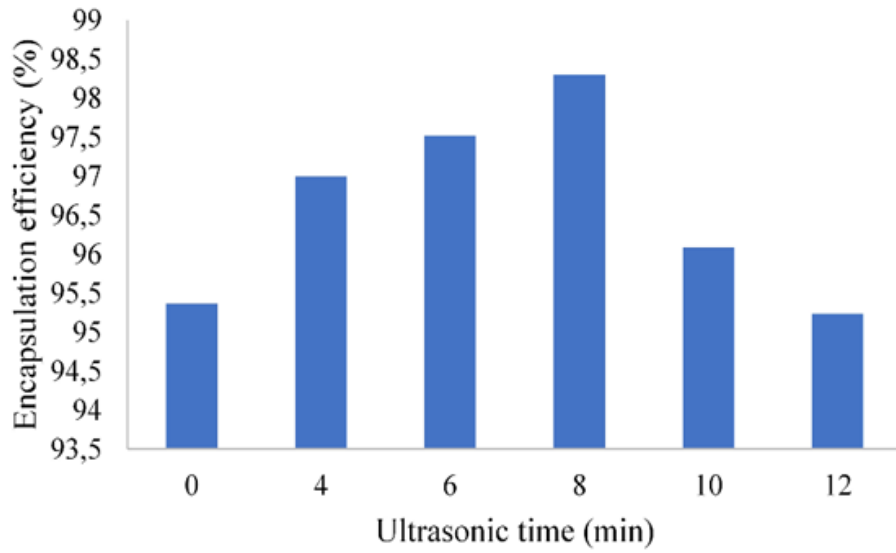


Figure 4. Effect ultrasonic time on encapsulation efficiency

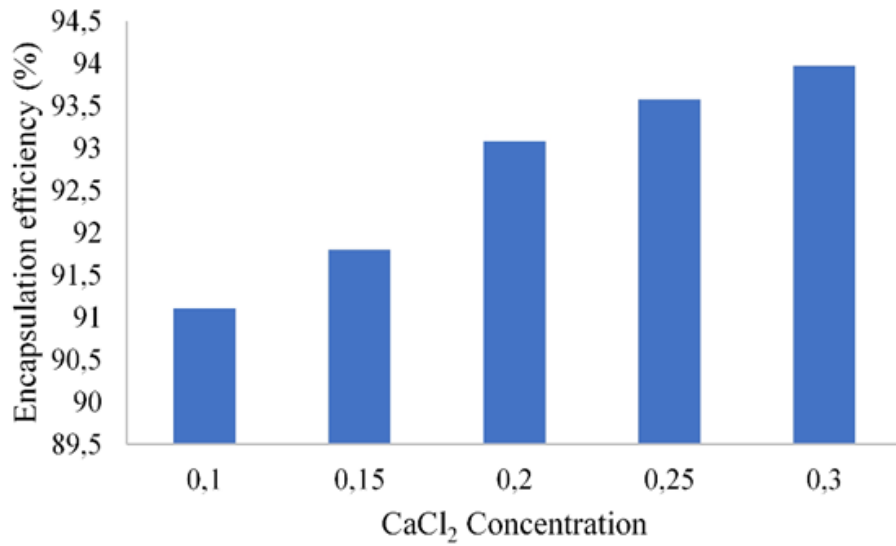


Figure 5. Effect CaCl₂ concentration on encapsulation efficiency

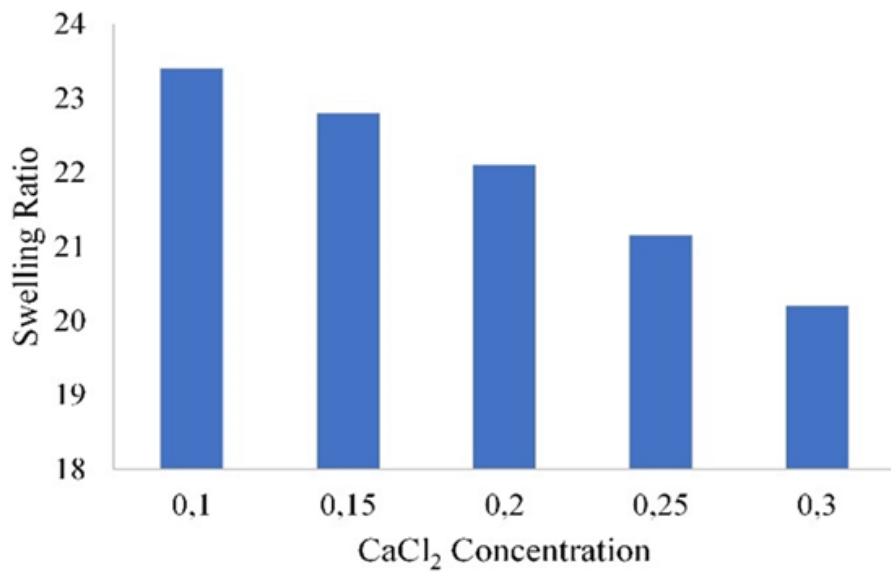


Figure 6. Effect of CaCl₂ concentration on swelling ratio

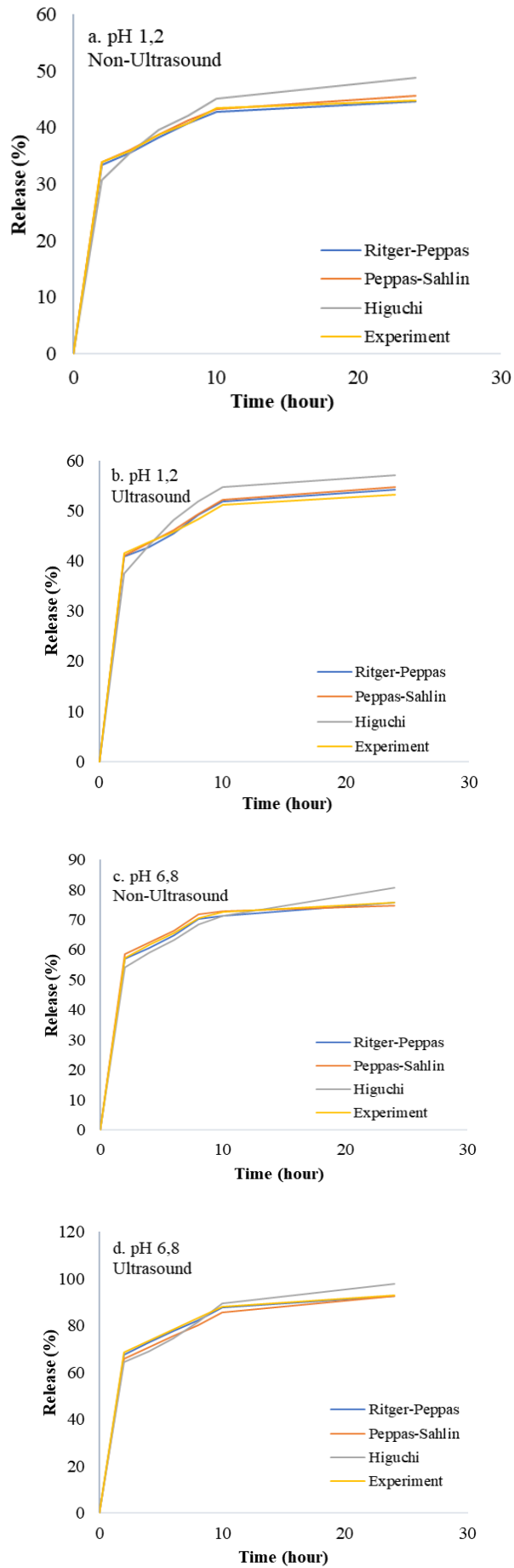


Figure 7. Curcumin release kinetic plot

Table 2: Release kinetics of bioactive curcumin

| System | Higuchi | | Ritger-Peppas | | | Peppas-Sahlin | | | | |
|-----------------------|---------|-------|---------------|-------|-------|---------------|-------|--------|-------|-------|
| | k_h | R^2 | k_1 | n | R^2 | k_1 | k_2 | m | R/F | R^2 |
| pH 1.2 | | | | | | | | | | |
| <i>Ultrasound</i> | 10,25 | 0,942 | 20,56 | 0,235 | 23,56 | 0,23 | 0,17 | 0,0089 | 0,996 | 23,56 |
| <i>Non-Ultrasound</i> | 9,91 | 0,953 | 13,11 | 0,342 | 17,47 | 0,17 | 0,18 | 0,0104 | 0,989 | 17,47 |
| pH 6.8 | | | | | | | | | | |
| <i>Ultrasound</i> | 20,56 | 0,982 | 48,47 | 0,158 | 50,12 | 0,01 | 0,17 | 0,0008 | 0,998 | 50,12 |
| <i>Non-Ultrasound</i> | 19,88 | 0,983 | 46,01 | 0,164 | 50,44 | 0,07 | 0,16 | 0,0017 | 0,997 | 50,44 |

Alginate has the potential to protect curcumin content in the gastric environment because it does not dissolve and dissociate under acidic conditions. The ultrasound-encapsulated beads (Figures b and d) had a faster ability to release than the non-ultrasound-encapsulated beads (Figures a and c), according to the release kinetics data. This is due to the fact that ultrasound treatment will cause the polymer bonds to break down, decreasing their ability to protect curcumin. Additionally, same tendency was observed in the study carried out by Wardhani et al. (2022) [32]. The kinetic parameters of hydrogel granules in alginate/carrageenan with ultrasound and non-ultrasound were determined based on data calculations with mathematical model equations of Ritger-Peppas, Peppas-Sahlin, and Higuchi. The Ritger-Peppas model and Peppas-Sahlin model were statistically the most effective models, as shown in Table 2. The high correlation coefficient values found in the Ritger-Peppas and Peppas-Sahlin models provide evidence of the best fit. Due to the fact that the majority of the bioactive causes are diffused, the Higuchi model has lower values when compared to the Ritger-Peppas and Peppas-Sahlin models. Since the Higuchi model's fitting value is less satisfactory than that of the Ritger-Peppas and Peppas-Sahlin models, the relaxation factor cannot be entirely excluded from the mechanism used by the curcumin compounds found in alginate/carrageenan beads. Similar conclusions may be obtained from the results of the Ritger-Peppas model that fits data the best, which shows that Fickian diffusion is the primary transmission mechanism throughout all hydrogel beads in the media with a case value of n 0.43. In addition, the Fickian diffusion in the polydisperse spherical delivery system is shown with a value of about 0.16. According to the experimental findings, ultrasonic hydrogel beads have a higher k_1 value than non-ultrasonic hydrogel beads (k_1 pH 1.2 = 13.11; k_1 pH 6.8 = 46.01). This indicates that the ultrasound-assisted release of bioactive particles is greater than the non-ultrasonic release of particles. Based on all hydrogel beads systems, data matching results using the Peppas-Sahlin equation showed small relaxation factor values but large Fickian diffusion values. The higher and more positive Peppas-Sahlin equation reaction rate constant (k_1) than the relaxation kinetic constant (k_2) indicates that Fickian diffusion dominates at pH 6.8, with the relaxation process having little effect on the release of Prasetyaningrum et al., 2023

bioactive curcumin. The contribution and relaxation of drug relaxation are shown by the R/F ratio. $R/F = 1$ generates a contribution that assists in both diffusion and erosion (relaxation). The dominant process is relaxation (erosion) when $R/F > 1$ and diffusion when $R/F < 1$. The R/F value of ultrasound beads (R/F pH 1.2 = 0.0089; R/F pH 6.8 = 0.0008) is smaller than that of non-ultrasound beads (R/F pH 1.2 = 0.0104; R/F pH 6.8 = 0.0017), which means that ultrasound beads have a higher F value than non-ultrasound beads. Compared to non-ultrasound, ultrasound has superior stability and is more dominant in diffusion, which impacts the release of bioactive beads. The decreased R/F value under ultrasound indicates that curcumin is more easily released from the degraded alginate/carrageenan as a result of the polymeric compound's chain breakage. When the polymer chains are broken by ultrasonic waves, alginate/carrageenan becomes more soluble. Degraded polymers therefore exhibit a decreased capacity to shield the bioactives they have been encapsulating and release them more quickly.

3.5. Swelling Analysis

Figure 6 shows that the swelling ratio of the beads decreases with increasing crosslinking agent concentration. Swelling ratio decreased with increasing concentration of $CaCl_2$. At a concentration of 0.1M $CaCl_2$ a swelling ratio of 23.4 was obtained and at a concentration of $CaCl_2$ of 0.3M a swelling ratio of 20.2 was obtained. This could be because increasing the concentration of the crosslinking agent results in the formation of more three-dimensional polymer networks with a high crosslinker density so that the swelling ratio will be lower in water [29]. Also, the concentration of the crosslinking agent affects the strength of the polymer beads. In Figure 6 it can be seen that the crosslinked beads with a crosslinker concentration of 0.1M had the highest swelling ratio and decreased with increasing crosslinker concentration. The lower the amount of crosslinking agent results in lower strength, so that the structure can expand while absorbing the medium. However, due to the low degree of crosslinking, the beads may break apart and dissolve in the medium [30]. In this study, with increasing $CaCl_2$ concentration, the number of Ca^{2+} ions per unit volume of liquid increased and more

Ca²⁺ would bind to the Alg chain. As a result, the work area will be less clean, which will result in less water entering the beads. In addition, the number of –COO– groups decreased due to the combination of Ca²⁺ and –COOH groups from Alg. Therefore, the electrostatic repulsion between the –CO– groups becomes weak, and this also causes a decrease in the swelling (%) of the beads [31].

4. Conclusions

In this study, ultrasound treatment was successfully used in the curcumin encapsulation process in Alg/Carr beads. The ultrasonication process is considered useful for protecting embedded bioactive components. FTIR spectra show that ultrasonication has little effect on curcumin encapsulation. The ultrasonication process causes a peak shift (1266 cm⁻¹) that triggers the breaking of the C-H bonds and results in polymer degradation. This phenomenon is also reflected in the SEM images which reveal that the microcapsules using ultrasound have a dark pores structure due to the cavitation phenomenon. PSA analysis showed that the ultrasound treatment resulted in a smaller particle size. Meanwhile, the encapsulation efficiency of curcumin in Alg/Carr increases to 95-98% in the presence of ultrasound treatment. The cavitation phenomenon in the sonication process causes polymer degradation which results in a decrease in particle size and an increase in encapsulation efficiency. In addition, the swelling ratio was also investigated and showed that the swelling ratio of the beads decreased with increasing concentration of the CaCl₂ crosslinking agent. Beads treated with ultrasound showed higher stability with a larger k₁ value for the Ritger-Peppas model and a smaller R/F ratio for the Peppas-Sahlin model indicating a diffusion-dominant mechanism of the bioactive release. Due to the breakage of the polymer compound chain, which is shown by a reduced R/F value on ultrasound, curcumin is more easily released from the degraded Alg/Carr.

Acknowledgments

The authors would like to express their gratitude to Diponegoro University for facilitating this research through RPIBT research funding with contract number 225-46/UN7.D2/PP/IV/2023.

References

- [1] V. Goëlo, M. Chaumon, A. Gonçalves, B.N. Estevinho, and F. Rocha. (2020). Polysaccharide-based delivery systems for curcumin and turmeric powder encapsulation using a spray-drying process. *Powder Technology*. 370: 137–146.
- [2] Q. Liu, Y. Jing, C. Han, H. Zhang, and Y. Tian. (2019). Encapsulation of curcumin in zein/caseinate/sodium alginate nanoparticles with improved physicochemical and controlled release properties. *Food Hydrocolloids*. 93: 432-442.
- [3] S.S. Patel, H.A. Pushpadass, M.E.E. Franklin, S.N. Battula, and P. Vellingiri. (2022). Microencapsulation of curcumin by spray drying: Characterization and fortification of milk. *Journal of Food Science and Technology*. 59(4): 1326-1340.
- [4] J. Lucas, M. Ralaivao, B.N. Estevinho, and F. Rocha. (2020). A new approach for the microencapsulation of curcumin by a spray drying method, in order to value food products. *Powder Technology*. 362: 428-435.
- [5] S.R. Bajaj, S.J. Marathe, and R.S. Singhal. (2021). Co-encapsulation of vitamins B12 and D3 using spray drying: Wall material optimization, product characterization, and release kinetics. *Food Chemistry*. 335: 127642.
- [6] L. Šturm, I.G.O. Črnivec, K. Istenič, A. Ota, P. Megušar, A. Slukan, M. Humar, S. Levic, V. Nedović, R. Kopinč, M. Deželak, G.A. Pereyra Gonzales, and U.N. Poklar. (2019). Encapsulation of non-dewaxed propolis by freeze-drying and spray-drying using gum Arabic, maltodextrin and inulin as coating materials. *Food and Bioproducts Processing*. 116: 196–211.
- [7] V. Šeregelj, G. Četković, J. Čanadanović-Brunet, V.T. Šaponjac, J. Vulić, S. Lević, and A. Hidalgo. (2021). Encapsulation of carrot waste extract by freeze and spray drying techniques: An optimization study. *LWT - Food Science and Technology*. 138: 110696.
- [8] L.L. Tan, K. Sampathkumar, J.H. Wong, and S.C.J. Loo. (2020). Divalent cations are antagonistic to survivability of freeze-dried probiotics encapsulated in cross-linked alginate. *Food and Bioproducts Processing*. 124: 369-377.
- [9] S. Atencio, A. Maestro, E. Santamaría, J.M. Gutiérrez, and C. González. (2020). Encapsulation of ginger oil in alginate-based shell materials. *Food Bioscience*. 37: 100714.
- [10] N. Pilipenko, O.H. Gonçalves, E. Bona, I.P. Fernandes, J.A. Pinto, G.D. Sorita, F.V. Leimann, and M.F. Barreiro. (2019). Tailoring swelling of alginate-gelatin hydrogel microspheres by crosslinking with calcium chloride combined with transglutaminase. *Carbohydrate Polymers*. 223: 115035.
- [11] S. Khanra, M. Mondal, G. Halder, O.N. Tiwari, K. Gayen, and T.K. Bhowmick. (2018). Downstream processing of microalgae for pigments, protein and carbohydrate in industrial application: A review. *Food and Bioproducts Processing*. 110: 60–84.
- [12] C. Bennacef, S. Desobry-Banon, L. Probst, and S. Desobry. (2021). Advances on alginate use for spherification to encapsulate biomolecules. *Food Hydrocolloids*. 118: 106782.
- [13] L. Gu, D.J. McClements, J. Li, Y. Su, Y. Yang, and J. Li. (2021). Formulation of alginate/carrageenan microgels to encapsulate, protect and release

- immunoglobulins: Egg Yolk IgY. *Food Hydrocolloids*. 112: 106349.
- [14] R.D. Barón, M.F. Valle-Vargas, G. Quintero-Gamero, M.X. Quintanilla-Carvajal, and J. Alean. (2021). Encapsulation of citrulline extract from watermelon (*Citrullus lanatus*) by-product using spray drying. *Powder Technology*. 385: 455-465.
- [15] L.E. Kurozawa and M.D. Hubinger. (2017). Hydrophilic food compounds encapsulation by ionic gelation. *Current Opinion in Food Science*. 15: 50–55.
- [16] T.S. Leong, G.J. Martin, and M. Ashokkumar. (2017). Ultrasonic encapsulation—a review. *Ultrasonics sonochemistry*. 35: 605-614.
- [17] N. Omer, Y.M. Choo, N. Ahmad, and N.S.M. Yusof. (2021). Ultrasound-assisted encapsulation of Pandan (*Pandanus amaryllifolius*) extract. *Ultrasonics Sonochemistry*. 79: 105793.
- [18] E.K. Silva, V.M. Azevedo, R.L. Cunha, M.D. Hubinger, and M.A.A. Meireles. (2016). Ultrasound-assisted encapsulation of annatto seed oil: Whey protein isolate versus modified starch. *Food Hydrocolloids*. 56: 71–83
- [19] M. Elgegren, S. Kim, D. Cordova, C. Silva, J. Noro, A. Cavaco-Paulo, and J. Nakamatsu. (2019). Ultrasound-Assisted Encapsulation of Sacha Inchi (*Plukenetia volubilis* Linneo.) Oil in Alginate-Chitosan Nanoparticles. *Polymers*. 11(8): 1245.
- [20] C.E. Iurciuc-Tincu, L.I. Atanase, L. Ochiuz, C. Jérôme, V. Sol, P. Martin, and M. Popa. (2020). Curcumin-loaded polysaccharides-based complex particles obtained by polyelectrolyte complexation and ionic gelation. I-Particles obtaining and characterization. *International Journal of Biological Macromolecules*. 147: 629–642.
- [21] F. Chen, L. Liu, and C. Tang. (2020). Spray-drying microencapsulation of curcumin nanocomplexes with soy protein isolate: Encapsulation, water dispersion, bioaccessibility and bioactivities of curcumin. *Food Hydrocolloids*. 105: 105821.
- [22] Q. Liang, X. Ren, X. Zhang, X. Hou, M. Chalamaiah, H. Ma, and B. Xu. (2018). Effect of ultrasound on the preparation of resveratrol-loaded zein particles. *Journal of Food Engineering*. 221: 88-94.
- [23] F. Yu, T. Cui, C. Yang, X. Dai, and J. Ma. (2019). K-Carrageenan/Sodium alginate double-network hydrogel with enhanced mechanical properties, anti-swelling, and adsorption capacity. *Chemosphere*. 237: 124417.
- [24] A. Prasetyaningrum, B.S. Wicaksono, A. Hakiim, A.D. Ashianti, S.F.C. Manalu, N. Rokhati, D.P. Utomo, and M. Djaeni. (2023). Ultrasound-Assisted Encapsulation of Citronella Oil in Alginate/Carrageenan Beads: Characterization and Kinetic Models. *ChemEngineering*. 7(1).
- [25] N. Pavlovic, J. Mijalkovic, V. Dordevi, D. Pecarski, B. Bugarski, and Z. Knezevic-Jugovic. (2022). Ultrasonication for production of nanoliposomes with encapsulated soy protein concentrate hydrolysate: Process optimization, vesicle characteristics and in vitro digestion. *Food Chemistry: X*. 15: 100370.
- [26] I. Tzanakis, M. Hodnett, G.S.B. Lebon, N. Dezhkunov, and D.G. Eskin. (2016). Calibration and performance assessment of an innovative high-temperature cavitometer. *Sensors and Actuators A: Physical*. 240: 57-69.
- [27] X. Luo, F. Fan, X. Sun, P. Li, T. Xu, J. Ding, and Y. Fang. (2022). Effect of ultrasonic treatment on the stability and release of selenium-containing peptide TSeMMM-encapsulated nanoparticles in vitro and in vivo. *Ultrasonics Sonochemistry*. 83: 105923.
- [28] A. Tunsirikongkon, Y. Pyo, D. Kim, P. Tran, and J. Park. (2020). Effect of calcium chloride on the protein encapsulation and stability of proliposomal granules. *Journal of Drug Delivery Science and Technology*. 57: 101672.
- [29] S. Yuan, K. Ning, and Y. He. (2020). Removal of copper ions using poly (acrylic acid-co-acrylamide) hydrogel microspheres with controllable size prepared by W/O Pickering emulsions. *Colloid and Polymer Science*. 298: 1465-1472.
- [30] E. Budianto, S.P. Muthoharoh, and N.M. Nizaro. (2015). Effect of Crosslinking Agents, pH and Temperature on Swelling Behavior of Cross-linked Chitosan Hydrogel. *Asian Journal of Applied Sciences*. 5(3).
- [31] S.M. Ibrahim, F.I. Abou El Fadl, and A.A. El-Naggar. (2014). Preparation and characterization of crosslinked alginate-CMC beads for controlled release of nitrate salt. *Journal of Radioanalytical and Nuclear Chemistry*. 299(3): 1531-1537.
- [32] D.H. Wardhani, F.N. Etnanta, H.N. Ulya, and N. Aryanti. (2022). Iron Encapsulation by Deacetylated Glucomannan as an Excipient Using the Gelation Method: Characteristics and Controlled Release. *Food Technology and Biotechnology*. 60(1): 41-51.